



Available online at <http://scik.org>

Commun. Math. Biol. Neurosci. 2024, 2024:37

<https://doi.org/10.28919/cmbn/8477>

ISSN: 2052-2541

A STUDY ON QUALITATIVE ANALYSIS OF A DISCRETE FRACTIONAL ORDER PREY-PREDATOR MODEL WITH INTRASPECIFIC COMPETITION

MD. JASIM UDDIN^{1,*}, M. B. ALMATRAFI², SHERAJUM MONIRA³

¹Department of Mathematics, University of Dhaka, Dhaka-1000, Bangladesh

²Department of Mathematics, College of Science, Taibah University, Al-Madinah Al-Munawarah, Saudi Arabia

³Department of Basic Sciences and Humanities, University of Asia Pacific, Dhaka, Bangladesh

Copyright © 2024 the author(s). This is an open access article distributed under the Creative Commons Attribution License, which permits unrestricted use, distribution, and reproduction in any medium, provided the original work is properly cited.

Abstract. The interaction of predators and prey is seen as a natural occurrence in biological systems. This paper investigates a predator-prey model with fractional derivatives. A term that models intraspecific competition within the predator population is also included in our proposed model with relation to the fractional derivative of Caputo. For large predator-to-prey density ratios, this extra term restricts the growth of the predator population. The topological structure of the fixed points is studied in this paper. Mathematically we prove that the considered model experiences both a Neimark-Sacker (NS) and a Period-doubling (PD) bifurcation under specific parametric conditions. We investigate the presence of a period-doubling bifurcation and a Neimark-Sacker bifurcation using the bifurcation theory. The dynamic behavior of this model is examined based on changes made to the control parameters and influenced by the initial conditions. The main features of numerical simulations, such as phase portraits, maximal Lyapunov exponents, and bifurcation diagrams, are shown to demonstrate the richer and more complicated dynamics, complex dynamical behaviors, and the accuracy of theoretical analysis. Furthermore, two methods of chaos management are applied in order to reduce the chaos that the system inherently contains.

Keywords: predator-prey system; Caputo fractional derivative; Period-Doubling(PD) and Neimark-Sacker (NS) bifurcations; Maximal Lyapunov Exponents (MLEs); chaos control.

2020 AMS Subject Classification: 39A28, 39A30, 39A33, 70K50, 92D25.

*Corresponding author

E-mail address: jasimu00@gmail.com

Received February 03, 2024

1. INTRODUCTION

Due to the fact that it occurs everywhere, the study of predator-prey interaction is a crucial field of study. Mathematical modeling has been used in a substantial number of articles to comprehend the intricate dynamics of the predator-prey system. Most dynamical systems are discussed using differential and difference equations. Many scholars have recently claimed that the population dynamics model is more relevant and realistic when difference equations are used to model it [1, 2, 3, 4]. Discrete-time systems are better ideal for organisms with non-overlapping generations, such as annual plants or insect colonies with a single generation each year. In lower-dimensional systems, the dynamics of discrete models are more complex than those of their continuous-time equivalents. Discrete systems best describe the more intricate patterns and chaotic behavior of nonlinear dynamics. For instance, a 1-dimensional discrete-time autonomous system can exhibit chaos, whereas a continuous-time system requires at least a 3-dimensional autonomous system [5].

One approach to discretizing a continuous system is to use the forward Euler scheme with an integral step size. Haderler and Gerstmann [6], Salman et al. [2], Cheng and Cao [7], Hu and Cao [1], Liu and Xiao [8], Ajaz et al. [4] and many others have used this discretization scheme and varied stepsize as a bifurcation parameter. An alternate discretization technique for differential equations known as piecewise constant arguments is presented in Din [3], Ishaque et al. [9], Khan [10], and the references therein. All the discretized systems proved the existence and singularity of positive steady states, the non-negativity and uniform boundedness of solution sets, as well as other properties that are difficult to prove when applying Euler's discretization method. Recently, some authors have switched from using traditional derivatives in discrete models to the well-known Caputo fractional derivative (we refer [11, 12, 13, 14, 29, 44]). Fractional-order models are more suitable than models with ordinary derivatives. Thus, research on fractional-order models has gained increasing importance, particularly in the field of biology. Moreover, the Caputo fractional derivative, involving the fractional order, is particularly crucial in these models as it enables the observation of memory effects. The models incorporating fractional-order present a more accurate representation of complex biological systems and

processes. This case causes significant advancements in our understanding of biological phenomena. The Caputo derivative additionally provides a strong and useful method for modelling fractional-order predator-prey interactions, ensuring the preservation of equilibrium states, and facilitating the application of conventional initial and boundary conditions for precise and insightful ecological predictions. It is a useful tool for examining intricate ecological dynamics in a variety of real-world issues due to its adaptability and capacity to capture memory effects [15]. Some dependence on previous states is required to elicit memory effects; however, the lack of a specific model for how memory combines information from the past may be shown as a limitation of the fractional derivative. On the other hand, we added to the considered model a fractional derivative approach to model memory as an effect distributed in time.

Several simple mathematical models have been put out to understand the interactions between prey and predator. Continuous-time population models, such as the Lotka-Volterra model [16, 17], have been employed in population dynamics, to comprehend the interactions of ecological species [18, 19, 20, 21, 22]. Populations in ecology have various methods to search for food and defend themselves, such as refuging, grouping, etc. In order to create mathematical models that are more precise, many ecological aspects and elements are included. The functional response in population dynamics must be considered in every prey-predator interaction. The functional response of the Holling type II is preferred to the other responses [23]. In [25] and [24], a discrete-time phytoplankton-zooplankton model with Holling type-II response was analyzed analytically and numerically, respectively, to examine the dynamics of a discrete-time predator-prey system with Holling-III type functional response. The authors investigate the stability, bifurcation, and chaos control of the discrete-time predator-prey model in [39] along with the Allee effect on the predator. The fixed point, local stability, types of bifurcations, and closed invariant curves for a fractional-order chemical reaction system have all been studied in [40]. The dynamics of a discrete-time predator-prey system using a functional response model of the Holling-III type are examined by the authors in [24]. A.Q. Khan et al. in [38] investigated global dynamics, Neimark-Sacker bifurcation, and hybrid control in Leslie's prey-predator model. An explicit bifurcation analysis criterion was provided for a three-dimensional system in [37]. The introduction of intraspecific competition within the predator population is the most significant

change we made to our model. When the ratio of predators to prey is noticeably high, there is intraspecific competition between the predator populations, which causes the predator population to experience decreased fitness as a result of food scarcity [41]. Blue crab populations exhibit intraspecific competition when they exhibit agonistic behavior, which injures them when there is a shortage of available prey [42]. Carnivorous fish (predators) eat detritivorous fish (prey) in the Sundarban mangrove habitat. Predators may readily catch prey and engage in intraspecific competition to obtain food since there is no sanctuary for the prey [43].

Some of the contributions that this research brings are as follows:

- (1) In the proposed model, there are two interdependent species, one of which provides food for the other. In this work, we examined the effects of intraspecific competition on the predator community within the model.
- (2) The stability of the proposed model is assessed by looking for possible fixed points.
- (3) It has been demonstrated that the proposed model can undergo both NS and PD bifurcations.
- (4) The proposed model has entered a chaotic state due to the Neimark-Sacker bifurcation; therefore, the OGY (Ott, Grebogi, and Yorke) and hybrid control procedures have been employed to regulate it.
- (5) We have included several numerical scenarios for our proposed fractional order discrete-time predator-prey model with intraspecific competition to confirm the validity of our theoretical results.

The remaining sections are arranged as follows: A discrete fractional order prey-predator model with intraspecific competition is present in Section 2. We examine the existence and local stability of fixed points in Section 3. The prospect of a period-doubling bifurcation at the coexistence fixed point of the discrete system is discussed in Section 4. The existence of Neimark-Sacker bifurcation around the system's coexistence fixed point is investigated in section 5. To bolster our analytical conclusions, we provide a quantitative depiction of the model dynamics in Section 6 together with phase portraits, bifurcation diagrams, and maximal Lyapunov exponents. In Section 7, the chaotic nature of the model is stabilized through

the application of OGY approaches and a hybrid control strategy. Section 8 offers succinct explanations.

2. MODEL FORMULATION

We assume that the prey and predator populations have constant densities through time, a uniform distribution across space, and no identifiable stage structure for either the prey or the predators. The proposed model is given by:

$$(1) \quad \begin{aligned} \dot{x} &= \delta_p x(1-x) - \phi_p xy, \\ \dot{y} &= \beta_p xy + (1 - \eta_p)y - \gamma_p y^2. \end{aligned}$$

Where prey and predator populations are represented by x and y , respectively, at any time t . All of the parameters $\delta_p, \phi_p, \beta_p, \eta_p, \gamma_p$ are positive constants with biological meanings. In the absence of a predator, the parameter δ_p is the intrinsic growth rate of prey populations with carrying capacity one. The predator's death rate is represented by η_p , and the predator's growth rate in the presence of prey is denoted by β_p . Also, η_p signifies the maximum rate of predation and γ_p denotes intraspecific competition within predator populations.

The Captuto fractional time derivative of a function $f(t)$ of order τ is given in [27] as follows.

$$(2) \quad D^\tau f(t) = \frac{1}{\Gamma(1-\tau)} \int_0^t \frac{1}{(t-\zeta_p)^\tau} f(\zeta_p) d\zeta_p,$$

where, $\tau \in (0, 1]$; $D^\tau = \frac{d^\tau}{dt^\tau}$, and $\Gamma(1-\tau)$ is the gamma function. As a result, the fractional-order version of the model (1) is as follows.

$$(3) \quad \begin{aligned} \frac{d^\tau x}{dt^\tau} &= D^\tau x = \delta_p x(1-x) - \phi_p xy, \\ \frac{d^\tau y}{dt^\tau} &= D^\tau y = \beta_p xy + (1 - \eta_p)y - \gamma_p y^2. \end{aligned}$$

The discretized version of the system(3) is presented here by using the Caputo fractional derivative.

$$(4) \quad \begin{aligned} x_{n+1} &= x_n + \frac{h^\tau}{\Gamma(\tau+1)} (\delta_p x_n(1-x_n) - \phi_p x_n y_n), \\ y_{n+1} &= y_n + \frac{h^\tau}{\Gamma(\tau+1)} (\beta_p x_n y_n + (1 - \eta_p)y_n - \gamma_p y_n^2). \end{aligned}$$

Note that the proposed predator-prey system with intraspecific competition looks the same as the Euler discretization if $\tau \rightarrow 1$ in (4). The proposed model contains drawbacks as well as advantages over the classical version. Since the proposed discrete model has only recently been developed, there is a lack of empirical evidence to confirm its accuracy and practical usefulness. Difference equations analysis and solution are more challenging than with typical discrete models. The proposed model parameters may be more unpredictable and challenging to determine than standard model parameters. Fractional order models can provide insight into intricate systems that incorporate memory effects and non-local interactions, despite these limitations. Fractional calculus focuses on integrals and derivatives of non-integer order. Fractional-order differential equations can describe complex dynamics, whereas integer-order models cannot.

3. EXISTENCE AND STABILITY ANALYSIS OF FIXED POINT

3.1. Existence of Fixed Points. The fixed points are $\tilde{\zeta}_0 = (0, 0)$, $\tilde{\zeta}_1 = (1, 0)$, $\tilde{\zeta}_2 = (0, \frac{1-\eta_p}{\gamma_p})$ and $\tilde{\zeta}_3 = (x^*, y^*)$, where $x^* = \frac{\gamma_p \delta_p + (-1 + \eta_p) \phi_p}{\gamma_p \delta_p + \beta_p \phi_p}$ and $y^* = \frac{\delta_p (1 + \beta_p - \eta_p)}{\gamma_p \delta_p + \beta_p \phi_p}$. The existence conditions of all the fixed points are given in the following table.

Fixed Points	Existence Conditions
$\tilde{\zeta}_0$	always
$\tilde{\zeta}_1$	always
$\tilde{\zeta}_2$	$\eta_p < 1$
$\tilde{\zeta}_3$	$(\beta_p - \eta_p) > -1$

3.2. Local stability analysis for fixed points. We assess the stability of system (4) at its identified fixed points. It is significant to note that the anticipated eigenvalues have an impact on the local stability of the fixed points, regardless of the magnitude of the expected eigenvalues at the fixed point $\tilde{\zeta}(x, y)$. Then

$$(5) \quad U(x, y) = \begin{pmatrix} \tilde{u}_{11} & \tilde{u}_{12} \\ \tilde{u}_{21} & \tilde{u}_{22} \end{pmatrix},$$

where

$$\tilde{u}_{11} = 1 + (\delta_p - 2x\delta_p - y\phi_p) \frac{h^\tau}{\Gamma(\tau + 1)},$$

$$\tilde{u}_{12} = -x\phi_p \frac{h^\tau}{\Gamma(\tau + 1)},$$

$$\tilde{u}_{21} = y\beta_p \frac{h^\tau}{\Gamma(\tau + 1)},$$

$$\tilde{u}_{22} = 1 + (1 + x\beta_p - 2y\gamma_p - \eta_p) \frac{h^\tau}{\Gamma(\tau + 1)}.$$

The following is how the characteristic equation can be stated at $\tilde{\zeta}(x, y)$:

$$(6) \quad F_{dd}(\lambda) := \lambda^2 - (2 + \tilde{\Delta}_{dd}\tilde{\mu}_{dd})\lambda + (1 + \tilde{\Delta}_{dd}\tilde{\mu}_{dd} + \tilde{\Omega}_{dd}\tilde{\mu}_{dd}^2) = 0$$

Here, we have

$$\tilde{\mu}_{dd} = \frac{h^\tau}{\Gamma(\tau + 1)},$$

$$\tilde{\Delta}_{dd} = 1 + x(\beta_p - 2\delta_p) + \delta_p - \eta_p - y(2\gamma_p + \phi_p)$$

$$\tilde{\Omega}_{dd} = -(-1 + 2x)\delta_p(1 + x\beta_p - 2y\gamma_p - \eta_p) + y(-1 + 2y\gamma_p + \eta_p)\phi_p$$

Therefore $F_{dd}(1) = \tilde{\Omega}_{dd}\tilde{\mu}_{dd}^2 > 0$ and $F_{dd}(-1) = 4 + 2\tilde{\Delta}_{dd}\tilde{\mu}_{dd} + \tilde{\Omega}_{dd}\tilde{\mu}_{dd}^2$.

Using Jury's criterion, the stability requirements of the following fixed points are specified.

We can find the jacobian matrix at $\tilde{\zeta}_0 = (0, 0)$ as

$$U(\tilde{\zeta}_0) = \begin{pmatrix} 1 + \delta_p\tilde{\mu}_{dd} & 0 \\ 0 & 1 + (1 - \eta_p)\tilde{\mu}_{dd} \end{pmatrix}$$

The eigenvalues of $U(\tilde{\zeta}_0)$ are $\lambda_1 = 1 + \delta_p\tilde{\mu}_{dd}$ and $\lambda_2 = 1 + (1 - \eta_p)\tilde{\mu}_{dd}$

Lemma 1. *The trivial fixed point $\tilde{\zeta}_0 = (0, 0)$ falls under the following topological classification.*

- (i) $\tilde{\zeta}_0$ is source if $h > \left(\frac{2}{\eta_p - 1}\Gamma(1 + \tau)\right)^{\frac{1}{\tau}}$,
- (ii) $\tilde{\zeta}_0$ is sink if $h < \left(\frac{2}{\eta_p - 1}\Gamma(1 + \tau)\right)^{\frac{1}{\tau}}$,
- (iii) $\tilde{\zeta}_0$ is non-hyperbolic if $h = \left(\frac{2}{\eta_p - 1}\Gamma(1 + \tau)\right)^{\frac{1}{\tau}}$.

The jacobian matrix at $\tilde{\zeta}_1 = (1, 0)$ is represented by

$$U(\tilde{\zeta}_1) = \begin{pmatrix} 1 - \delta_p \mu_{dd} & -\phi_p \mu_{dd} \\ 0 & 1 + (1 + \beta_p - \eta_p) \mu_{dd} \end{pmatrix}.$$

The eigenvalues of $U(\tilde{\zeta}_1)$ are $\lambda_1 = 1 - \delta_p \mu_{dd}$ and $\lambda_2 = 1 + (1 + \beta_p - \eta_p) \mu_{dd}$.

Lemma 2. *The predator-free fixed point $\tilde{\zeta}_1$ falls under the following topological classification:*

- (i) $\tilde{\zeta}_1$ is source if $h > \left(\frac{2}{\eta_p - \beta_p - 1} \Gamma(1 + \tau)\right)^{\frac{1}{\tau}}$,
- (ii) $\tilde{\zeta}_1$ is sink if $h < \left(\frac{2}{\eta_p - \beta_p - 1} \Gamma(1 + \tau)\right)^{\frac{1}{\tau}}$,
- (iii) $\tilde{\zeta}_1$ is non-hyperbolic if $h = \left(\frac{2}{\eta_p - \beta_p - 1} \Gamma(1 + \tau)\right)^{\frac{1}{\tau}}$,

The jacobian matrix changes when we reach $\tilde{\zeta}_2 = (0, \frac{1 - \eta_p}{\gamma_p})$ which is given as follows:

$$U(\tilde{\zeta}_2) = \begin{pmatrix} \frac{\gamma_p + (\gamma_p \delta_p + (-1 + \eta_p) \phi_p) \mu_{dd}}{\gamma_p} & 0 \\ -\frac{\beta_p (-1 + \eta_p) \mu_{dd}}{\gamma_p} & 1 + (1 - \eta_p) \mu_{dd} \end{pmatrix}$$

The eigenvalues of $U(\tilde{\zeta}_2)$ are $\lambda_1 = 1 + (-1 + \eta_p) \mu_{dd}$ and $\lambda_2 = \frac{\gamma_p + (\gamma_p \delta_p + (-1 + \eta_p) \phi_p) \mu_{dd}}{\gamma_p}$.

Lemma 3. *The prey-free fixed point $\tilde{\zeta}_2 = (0, \frac{1 - \eta_p}{\gamma_p})$ can be classified according to the topology in the following manner:*

- (i) if $\eta_p > -1$ then the fixed point $\tilde{\zeta}_2 = (0, \frac{1 - \eta_p}{\gamma_p})$ is
 - (i.i) $\tilde{\zeta}_2$ is sink if $0 < h < \min\left\{\left(\frac{2}{\eta_p - 1} \Gamma(1 + \tau)\right)^{\frac{1}{\tau}}, \left(\frac{-2\gamma_p}{\gamma_p \delta_p + (-1 + \eta_p) \phi_p} \Gamma(1 + \tau)\right)^{\frac{1}{\tau}}\right\}$,
 - (i.ii) $\tilde{\zeta}_2$ is source if $h > \max\left\{\left(\frac{2}{\eta_p - 1} \Gamma(1 + \tau)\right)^{\frac{1}{\tau}}, \left(\frac{-2\gamma_p}{\gamma_p \delta_p + (-1 + \eta_p) \phi_p} \Gamma(1 + \tau)\right)^{\frac{1}{\tau}}\right\}$,
 - (i.iii) $\tilde{\zeta}_2$ is non-hyperbolic if $h = \left(\frac{2}{\eta_p - 1} \Gamma(1 + \tau)\right)^{\frac{1}{\tau}}$ or $h = \left(\frac{-2\gamma_p}{\gamma_p \delta_p + (-1 + \eta_p) \phi_p} \Gamma(1 + \tau)\right)^{\frac{1}{\tau}}$,
- (ii) if $\eta_p < -1$ then the fixed point $\tilde{\zeta}_2 = (0, \frac{1 - \eta_p}{\gamma_p})$ is
 - (ii.i) $\tilde{\zeta}_2$ is source if $h > \left(\frac{2}{\delta_p} \Gamma(1 + \tau)\right)^{\frac{1}{\tau}}$,
 - (ii.ii) $\tilde{\zeta}_2$ is saddle if $h < \left(\frac{2}{\delta_p} \Gamma(1 + \tau)\right)^{\frac{1}{\tau}}$,
 - (ii.iii) $\tilde{\zeta}_2$ is non-hyperbolic if $h = \left(\frac{2}{\delta_p} \Gamma(1 + \tau)\right)^{\frac{1}{\tau}}$,
- (iii) if $\eta_p = -1$ then the fixed point $\tilde{\zeta}_2 = (0, \frac{1 - \eta_p}{\gamma_p})$ is non-hyperbolic.

At $\tilde{\zeta}_3(x^*, y^*)$,

$$\Delta_{dd4}^{\sim} = \Delta_{dd}^{\sim}|_{x=x^*, y=y^*},$$

$$\Omega_{dd4}^{\sim} = \Omega_{dd}^{\sim}|_{x=x^*, y=y^*}.$$

Regarding the stability requirements of $\tilde{\zeta}_3(x^*, y^*)$, we provide the following lemma.

Lemma 4. *The co-existence fixed point $\tilde{\zeta}_3(x^*, y^*)$ can be categorized according to the following topological rules:*

(i) $\tilde{\zeta}_3$ is source if

$$(i.i) \Delta_{dd4}^{\sim 2} - 4\Omega_{dd4}^{\sim} \geq 0 \text{ and } \mu_{dd}^{\sim} > \frac{-\Delta_{dd4}^{\sim} + \sqrt{\Delta_{dd4}^{\sim 2} - 4\Omega_{dd4}^{\sim}}}{\Omega_{dd4}^{\sim}}$$

$$(i.ii) \Delta_{dd4}^{\sim 2} - 4\Omega_{dd4}^{\sim} < 0 \text{ and } \mu_{dd}^{\sim} > \frac{-\Delta_{dd4}^{\sim}}{\Omega_{dd4}^{\sim}}$$

(ii) $\tilde{\zeta}_3$ is sink if

$$(ii.i) \Delta_{dd4}^{\sim 2} - 4\Omega_{dd4}^{\sim} \geq 0 \text{ and } \mu_{dd}^{\sim} < \frac{-\Delta_{dd4}^{\sim} - \sqrt{\Delta_{dd4}^{\sim 2} - 4\Omega_{dd4}^{\sim}}}{\Omega_{dd4}^{\sim}}$$

$$(ii.ii) \Delta_{dd4}^{\sim 2} - 4\Omega_{dd4}^{\sim} < 0 \text{ and } \mu_{dd}^{\sim} < \frac{-\Delta_{dd4}^{\sim}}{\Omega_{dd4}^{\sim}}$$

(iii) $\tilde{\zeta}_3$ is non-hyperbolic if

$$(iii.i) \Delta_{dd4}^{\sim 2} - 4\Omega_{dd4}^{\sim} \geq 0 \text{ and } \mu_{dd}^{\sim} = \frac{-\Delta_{dd4}^{\sim} \pm \sqrt{\Delta_{dd4}^{\sim 2} - 4\Omega_{dd4}^{\sim}}}{\Omega_{dd4}^{\sim}}; \mu_{dd}^{\sim} \neq \frac{-2}{\Delta_{dd4}^{\sim}}, \frac{-4}{\Delta_{dd4}^{\sim}}$$

$$(iii.ii) \Delta_{dd4}^{\sim 2} - 4\Omega_{dd4}^{\sim} < 0 \text{ and } \mu_{dd}^{\sim} = \frac{-4}{\Delta_{dd4}^{\sim}}.$$

(iv) $\tilde{\zeta}_3$ is saddle if otherwise

Let,

$$\widehat{PBF}_{\tilde{\zeta}_3}^{1,2} = \left\{ (\delta_p, \phi_p, \eta_p, \beta_p, \gamma_p, \tau, h) : h = \left(\frac{-\Delta_{dd4}^{\sim} \pm \sqrt{\Delta_{dd4}^{\sim 2} - 4\Omega_{dd4}^{\sim}}}{\Omega_{dd4}^{\sim}} \Gamma(1 + \tau) \right)^{\frac{1}{\tau}} = h_{\pm} \right\}.$$

with $\Delta_{dd4}^{\sim 2} - 4\Omega_{dd4}^{\sim} \geq 0, \mu_{dd}^{\sim} \neq \frac{-2}{\Delta_{dd4}^{\sim}}, \frac{-4}{\Delta_{dd4}^{\sim}}$. When the parameters $(\delta_p, \phi_p, \eta_p, \beta_p, \gamma_p, \tau, h)$ change within a constrained region of $\widehat{PBF}_{\tilde{\zeta}_3}^{1,2}$, the system (4) at $\tilde{\zeta}_3$ experiences a PD bifurcation. Also,

let

$$\widehat{NBF}_{\tilde{\zeta}_3} = \left\{ (\delta_p, \phi_p, \eta_p, \beta_p, \gamma_p, \tau, h) : h = \left(\Gamma(1 + \tau) \frac{-\Delta_{dd4}^{\sim}}{\Omega_{dd4}^{\sim}} \right)^{\frac{1}{\tau}} = h_{NS}, \Delta_{dd4}^{\sim 2} - 4\Omega_{dd4}^{\sim} < 0 \right\}.$$

An NS bifurcation will occur in system (4) if the parameters $(\delta_p, \phi_p, \eta_p, \beta_p, \gamma_p, \tau, h)$ vary around the set $\widehat{NBF}_{\tilde{\zeta}_3}$.

4. PERIOD-DOUBLING BIFURCATION

The emphasis of this section is on the existence of a period-doubling bifurcation at a positive equilibrium point $\tilde{\zeta}_3(x^*, y^*)$ of the system (4). This type of bifurcation is explored after demonstrating its presence and direction using normal forms. Several experts have recently studied the period-doubling bifurcation in discrete-time mathematical models [28, 30, 31].

The parameters $(\delta_p, \phi_p, \eta_p, \beta_p, \gamma_p, \tau, h)$, are randomly chosen to locate in $\widehat{PBF}_{\tilde{\zeta}_3}^{1,2}$. Take into consideration system (4) at $\tilde{\zeta}_3(x^*, y^*)$, the equilibrium point. Let

$$h = h_- = \left(\frac{-\Delta_{dd4} - \sqrt{\Delta_{dd4}^2 - 4\Omega_{dd4}}}{\Omega_{dd4}} \Gamma(1 + \tau) \right)^{\frac{1}{\tau}}.$$

Additionally, the eigenvalues of $U(\tilde{\zeta}_3)$ are provided as

$$\lambda_1(h_-) = -1, \text{ and } \lambda_2(h_-) = \lambda^{**}$$

For $|\lambda_2(h_-) \neq 1|$ to be implied

$$(7) \quad \lambda^{**} \neq \pm 1.$$

Next, we set $A(h_-) = U(x^*, y^*)$ and apply the transformations $\hat{x} = x - x^+, \hat{y} = y - y^+$. We move the fixed point of the system (4) to the initial position. As a result, system (4) can be written as

$$(8) \quad \begin{pmatrix} \hat{x} \\ \hat{y} \end{pmatrix} \rightarrow A(h_-) \begin{pmatrix} \hat{x} \\ \hat{y} \end{pmatrix} + \begin{pmatrix} F_{x1}(\hat{x}, \hat{y}, h_-) \\ F_{x2}(\hat{x}, \hat{y}, h_-) \end{pmatrix},$$

where $X = (\hat{x}, \hat{y})^T$ and

$$(9) \quad \begin{aligned} F_{x1}(\hat{x}, \hat{y}, h_+) &= \frac{1}{2} (-2\hat{x}^2 \delta_p \mu_{dd} - 2\hat{x}\hat{y} \phi_p \mu_{dd}), \\ F_{x2}(\hat{x}, \hat{y}, h_+) &= \frac{1}{2} (2\hat{x}\hat{y} \beta_p \mu_{dd} - 2\hat{y}^2 \gamma_p \mu_{dd}). \end{aligned}$$

It is feasible to express system (4) as

$$X_{n+1} = AX_n + \frac{1}{2}B_e(X_n, X_n) + \frac{1}{6}C_e(X_n, X_n, X_n) + O(\|X_n\|^4)$$

As symmetric multi-linear vector functions on $x, y, u \in \mathbb{R}^2$, $B_e(x, y) = \begin{pmatrix} B_{e1}(x, y) \\ B_{e2}(x, y) \end{pmatrix}$ and

$C_e(x, y, u) = \begin{pmatrix} C_{e1}(x, y, u) \\ C_{e2}(x, y, u) \end{pmatrix}$ are defined as follows:

$$B_{e1}(x, y) = \sum_{j,k=1}^2 \frac{\delta^2 F_{x1}(\xi, h)}{\delta \xi_j \delta \xi_k} \Bigg|_{\xi=0} \quad x_j y_k = -\tilde{\mu}_{dd} (2x_1 y_1 \delta_p + x_2 y_1 \phi_p + x_1 y_2 \phi_p),$$

$$B_{e2}(x, y) = \sum_{j,k=1}^2 \frac{\delta^2 F_{x2}(\xi, h)}{\delta \xi_j \delta \xi_k} \Bigg|_{\xi=0} \quad x_j y_k = \tilde{\mu}_{dd} (x_2 y_1 \beta_p + x_1 y_2 \beta_p - 2x_2 y_2 \gamma_p).$$

and

$$C_{e1}(x, y, u) = \sum_{j,k,l=1}^2 \frac{\delta^3 F_{x1}(\xi, h)}{\delta \xi_j \delta \xi_k \delta \xi_l} \Bigg|_{\xi=0} \quad x_j y_k u_l = 0,$$

$$C_{e2}(x, y, u) = \sum_{j,k,l=1}^2 \frac{\delta^3 F_{x1}(\xi, h)}{\delta \xi_j \delta \xi_k \delta \xi_l} \Bigg|_{\xi=0} \quad x_j y_k u_l = 0.$$

The two eigenvectors associated with A and A^T with eigenvalue $\lambda_1(h_-) = -1$ should be represented by $\tilde{q}_a, \tilde{q}_b \in \mathbb{R}^2$ such that $A(h_-)\tilde{q}_a = -\tilde{q}_a$ and $A^T(h_-)\tilde{q}_b = -\tilde{q}_b$. Therefore, by performing simple calculations, we arrive at

$$\tilde{q}_a = \begin{pmatrix} q_{a11} \\ 1 \end{pmatrix},$$

$$\tilde{q}_b = \begin{pmatrix} q_{b11} \\ 1 \end{pmatrix}.$$

where

$$q_{a11} = \frac{(-1 + 2y^* \gamma_p + \delta_p - x^* (\beta_p + 2\delta_p) + \eta_p - y^* \phi_p)}{2y^* \beta_p} - \frac{\sqrt{(x^{*2} (\beta_p + 2\delta_p)^2 + (-1 + 2y^* \gamma_p + \delta_p + \eta_p - y^* \phi_p)^2 + A_{pp1})}}{2y^* \beta_p}$$

$$q_{b11} = \frac{(-1 - 2y^* \gamma_p - \delta_p + x^* (\beta_p + 2\delta_p) - \eta_p + y^* \phi_p)}{2x^* \beta_p} + \frac{\sqrt{(x^{*2} (\beta_p + 2\delta_p)^2 + (-1 + 2y^* \gamma_p + \delta_p + \eta_p - y^* \phi_p)^2 + A_{pp2})}}{2x^* \beta_p}$$

$$A_{pp1}^{\sim} = -2x^*(2\delta_p(-1+2y^*\gamma_p+\delta_p+\eta_p-y^*\phi_p)+\beta_p(-1+2y^*\gamma_p+\delta_p+\eta_p+y^*\phi_p))$$

$$A_{pp2}^{\sim} = -2x^*(2\delta_p(-1+2y^*\gamma_p+\delta_p+\eta_p-y^*\phi_p)+\beta_p(-1+2y^*\gamma_p+\delta_p+\eta_p+y^*\phi_p)).$$

To get $\langle \tilde{q}_a, \tilde{q}_b \rangle = 1$, where $\langle \tilde{q}_a, \tilde{q}_b \rangle = q_{a11}\tilde{q}_{b11} + q_{a12}\tilde{q}_{b12}$, we must make use of the normalized vector $\tilde{q}_b = \vartheta_+ \tilde{q}_b$, with $\vartheta_+ = \frac{1}{1-q_{a11}\tilde{q}_{b11}}$. We must examine the sign of $s_a(h_-)$, the coefficient of the critical standard form[32], to determine the direction of the PD bifurcation.

$$(10) \quad s_1(h_-) = \frac{1}{6} \langle \tilde{q}_b, C_e(\tilde{q}_a, \tilde{q}_a, \tilde{q}_a) \rangle - \frac{1}{2} \langle \tilde{q}_b, B_e(\tilde{q}_b, (A-I)^{-1}B_e(\tilde{q}_a, \tilde{q}_a)) \rangle$$

The direction and stability of PD bifurcation can be shown using the following theorem in light of the justification presented above.

Theorem 1. *For the fixed point $\tilde{\xi}_3(x^*, y^*)$, assume that Eq.(7) is valid. If $s_1(h_-) \neq 0$ and h_- fluctuate its value in a constrained vicinity to $\widehat{PBF}_{\tilde{\xi}_3}^{1,2}$, system (4) will experience a period-doubling bifurcation at $\tilde{\xi}_3(x^*, y^*)$. Additionally, if $s_1(h_-)$ is positive or negative, period-2 orbits split apart from $\tilde{\xi}_3(x^*, y^*)$ and become stable (or unstable).*

5. NEIMARK-SACKER BIFURCATION

This section investigates the Neimark-Sacker bifurcation around the positive equilibrium point $\tilde{\xi}_3(x^*, y^*)$ of the system (4). We used the conventional concept of bifurcation to determine the direction and presence of this form of bifurcation. Several mathematicians have recently investigated the Neimark-Sacker bifurcation, which is linked to a number of discrete-time mathematical systems [33, 34, 36].

Assume the parameters $(\delta_p, \phi_p, \eta_p, \beta_p, \gamma_p, \tau, h) \in \widehat{NBF}_{\tilde{\xi}_3}$ then the eigenvalues of system (4) are $\lambda_{1,2} \in \mathbb{C}$.

$$h = h_{NS} = \left(\Gamma(1+\tau) \frac{-\Delta_{dd4}}{\Omega_{dd4}} \right)^{\frac{1}{\tau}}$$

Also,

$$(11) \quad \frac{d|\lambda_i(h)|}{dh} \Big|_{h=h_{NS}} = \frac{\gamma_p^2 \delta_p (\gamma_p (1+\beta_p+\delta_p-\eta_p) + (-1+\eta_p)\phi_p)}{2(\gamma_p \delta_p + \beta_p \phi_p)(\gamma_p \delta_p + (-1+\eta_p)\phi_p)^2} \neq 0$$

$$-(trU(h_{NS})) \neq 0 \Rightarrow \frac{(\gamma_p^2 \delta_p (\beta_p^2 + \delta_p^2 - 2\beta_p(-1+\eta_p) + (-1+\eta_p)^2) - 2\gamma_p \delta_p (\beta_p + \beta_p^2 + \delta_p - \beta_p \eta_p - \delta_p \eta_p) \phi_p + \Lambda_{p1})}{((1+\beta_p-\eta_p)(\gamma_p \delta_p + \beta_p \phi_p)(\gamma_p \delta_p (-1+\eta_p)\phi_p))} \neq 0, 1.$$

where $\Lambda_{p1} = (-2\beta_p^2 + 2\beta_p(-1+\eta_p) + \delta_p(-1+\eta_p))(-1+\eta_p)\phi_p^2$.

and

$$(12) \quad \lambda^k(h_{NS}) \neq 1; k = 1, 2, 3, 4$$

Take into account the scenario in which $\tilde{q}_a, \tilde{q}_b \in \mathbb{R}^2$ are the two eigenvectors of $A(h_{NS})$ and $A^T(h_{NS})$ with respect to the eigenvalues $\lambda(h_{NS})$ and $\bar{\lambda}(h_{NS})$ in such a way

$$(13) \quad \begin{aligned} A(h_{NS})\tilde{q}_a &= \lambda(h_{NS})\tilde{q}_a, & A(h_{NS})\bar{\tilde{q}}_a &= \bar{\lambda}(h_{NS})\bar{\tilde{q}}_a, \\ A^T(h_{NS})\tilde{q}_b &= \bar{\lambda}(h_{NS})\tilde{q}_b, & A^T(h_{NS})\bar{\tilde{q}}_b &= \lambda(h_{NS})\bar{\tilde{q}}_b. \end{aligned}$$

Therefore, by performing simple calculations, we find:

$$\begin{aligned} \tilde{q}_a &= \begin{pmatrix} q_{\tilde{a}11} \\ 1 \end{pmatrix}, \\ \tilde{q}_b &= \begin{pmatrix} q_{\tilde{b}11} \\ 1 \end{pmatrix}. \end{aligned}$$

To obtain $\langle \tilde{q}_a, \tilde{q}_b \rangle = 1$, where $\langle \tilde{q}_a, \tilde{q}_b \rangle = q_{\tilde{a}11}q_{\tilde{b}11} + q_{\tilde{a}12}q_{\tilde{b}12}$, we set the normalized vector $\tilde{q}_b = \vartheta_{NS}\tilde{q}_b$, with $\vartheta_{NS} = \frac{1}{1+q_{\tilde{b}11}q_{\tilde{a}11}}$.

By taking into account how h can fluctuate close to h_{NS} and for $z \in \mathbb{C}$, we can decompose $X \in \mathbb{R}^2$ as $X = z\tilde{q}_a + \bar{z}\bar{\tilde{q}}_a$. $z = \langle \tilde{q}_b, X \rangle$ is the exact formulation of z . Thus, for $|h|$ close to h_{NS} , system (4) switched to the following system:

$$(14) \quad z \longmapsto \bar{\mu}(h)z + \hat{h}(z, \bar{z}, h),$$

where $\mu(h) = (1 + \hat{\varphi}(h))e^{i\theta(h)}$ with $\hat{\varphi}(h_{NS}) = 0$ and $\hat{h}(z, \bar{z}, h)$ is an easily computed complex-valued function. When Taylor expansion is used on the function \hat{h} , we have

$$\hat{h}(z, \bar{z}, h) = \sum_{k+l \geq 2} \frac{1}{k!l!} \hat{h}_{kl}(h) z^k \bar{z}^l \quad \text{with} \quad \hat{h}_{kl} \in \mathbb{C}, k, l = 0, 1, \dots$$

The Taylor coefficients are defined as follows.

$$(15) \quad \begin{aligned} \hat{h}_{20}(h_{NS}) &= \langle \tilde{q}_b, B_e(\tilde{q}_a, \tilde{q}_a) \rangle, \\ \hat{h}_{11}(h_{NS}) &= \langle \tilde{q}_b, B_e(\tilde{q}_a, \bar{\tilde{q}}_a) \rangle, \\ \hat{h}_{02}(h_{NS}) &= \langle \tilde{q}_b, B_e(\bar{\tilde{q}}_a, \bar{\tilde{q}}_a) \rangle, \\ \hat{h}_{21}(h_{NS}) &= \langle \tilde{q}_b, C_e(\tilde{q}_a, \tilde{q}_a, \bar{\tilde{q}}_a) \rangle \end{aligned}$$

The sign of the first Lyapunov coefficient $s_2(h_{NS})$ indicates the direction of the NS bifurcation, which is given by the expression

$$(16) \quad s_2(h_{NS}) = \operatorname{Re} \left(\frac{\lambda_2 \widehat{h}_{21}}{2} \right) - \operatorname{Re} \left(\frac{(1-2\lambda_1)\lambda_2^2 \widehat{h}_{20} \widehat{h}_{11}}{2(1-\lambda_1)} \right) - \frac{1}{2} \left| \widehat{h}_{11} \right|^2 - \frac{1}{4} \left| \widehat{h}_{02} \right|^2$$

In the light of the preceding explanation, the following theorem can be utilized to show the direction and stability of NS bifurcation.

Theorem 2. *Assume that Eq.(11) is true and that $s_2(h_{NS}) \neq 0$ is true. If the value of h fluctuates in a specific area around \widehat{NBF}_{ξ_3} , then system (4) experiences a Neimark-Sacker bifurcation at $\tilde{\zeta}_3(x^*, y^*)$. Additionally, if $s_2(h_{NS})$ is negative (resp. positive) and the NS bifurcation is supercritical (resp. sub-critical), a unique invariant closed curve that is attracting (resp. repelling) bifurcates from $\tilde{\zeta}_3(x^*, y^*)$ as well.*

6. NUMERICAL STUDY

In order to validate our theoretical conclusions and highlight some unexpected, intriguing complex dynamical behaviors present in system (4), some numerical simulations are presented to display bifurcation diagrams, phase portraits, and maximal Lyapunov exponents of the system (4). To investigate the PD and NS bifurcations for the unique positive fixed point $\tilde{\zeta}_3(x^*, y^*)$, one can examine the initial condition (x_0, y_0) situated around the fixed point. We consider the bifurcation parameters in the following scenarios:

Scenario (i): The following parameter values were chosen: $\eta_p = 1.7$, $\beta_p = 1.26$, $\delta_p = 3.06$, $\phi_p = 1.05$, $\gamma_p = 0.9$, $\tau = 0.5896$ and h varies between $0.55 \leq h \leq 0.8$. We arrive at a fixed point $\tilde{\zeta}_3(x^*, y^*) = (0.855776, 0.420309)$ and a point $h_- = 0.6179$ for PD bifurcation. The estimated eigenvalues are $\lambda_{1,2} = -1, 0.482685$. The symmetric multilinear functions is defined as follows

$$B_{e1}(x, y) = (-5.14054x_1y_1 - 0.881956x_2y_1 - 0.881956x_1y_2),$$

$$B_{e2}(x, y) = (1.05835x_2y_1 + 1.05835x_1y_2 - 1.51192x_2y_2).$$

and

$$C_{e1}(x, y, u) = 0,$$

$$C_{e2}(x, y, u) = 0.$$

Let the two eigenvectors of $A(h_-)$ and $A^T(h_-)$, be $\tilde{q}_a, \tilde{q}_b \in \mathbb{R}^2$ which correspond to $\lambda_{1,2}$. Therefore, $\tilde{q}_a \sim (-0.966772, 0.255639)^T$ and $\tilde{q}_b \sim (-0.91238, -0.409345)^T$. For $\langle \tilde{q}_a, \tilde{q}_b \rangle = 1$, after which the normalized vector can be used as $\tilde{q}_b = \vartheta_+ \tilde{q}_b$ where, $\vartheta_+ = 1.28631$. Then, we obtain

$$\tilde{q}_a \sim (-0.966772, 0.255639)^T \text{ and } \tilde{q}_b \sim (-1.1736, -0.526543)^T.$$

The Lyapunov coefficient $s_1(h_-) = 2.94871 > 0$ is obtained from (10). Consequently, the PD bifurcation is sub-critical, and Theorem 1 is established.

The trajectories of the model are depicted in Figure 1 (a-b) as evolving from a fixed point to a chaotic attractor via a PD bifurcation. Figure 1(c) depicts the estimated MLEs for Figure 1 (a-b). The phase portraits are presented in Figure 2 to illustrate the presented bifurcation in Figure 1, which essentially demonstrates the bifurcation of a smooth, invariant closed curve into a chaotic attractor from a stable fixed point.

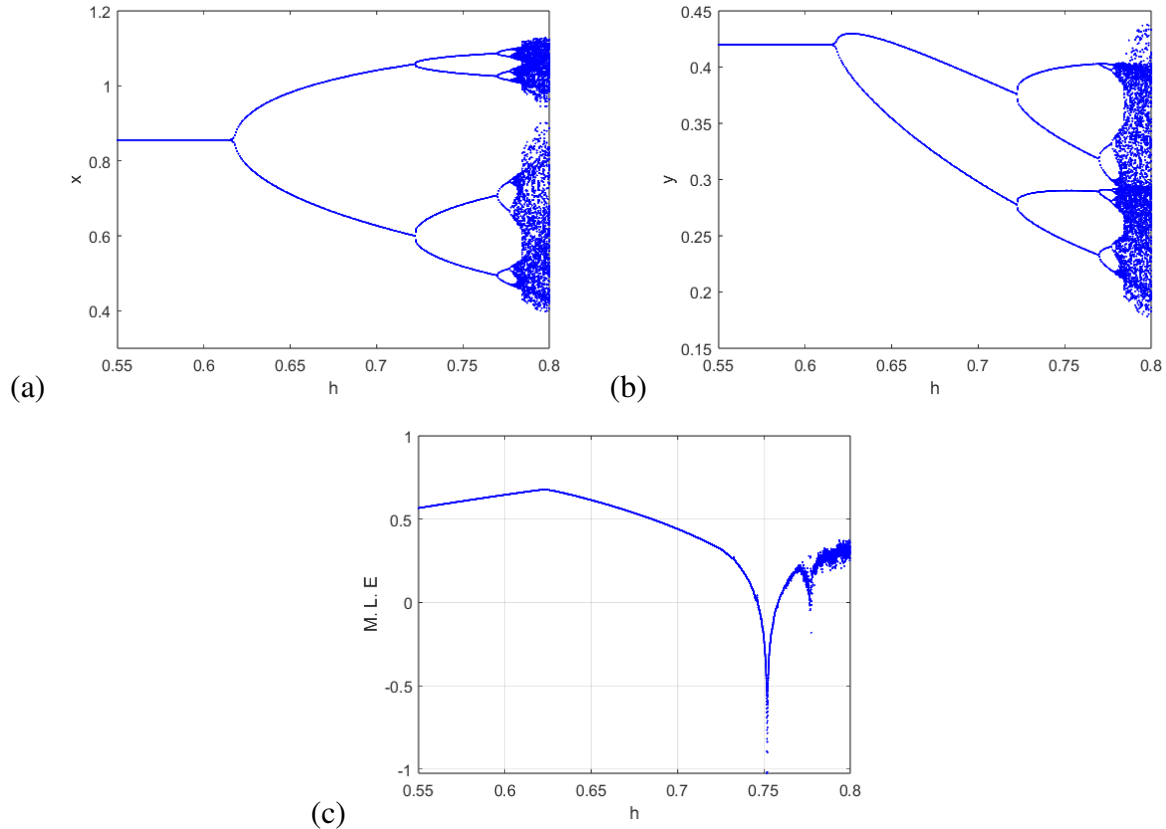


FIGURE 1. Visualisation of PD bifurcation and MLEs of species for changing parameter h

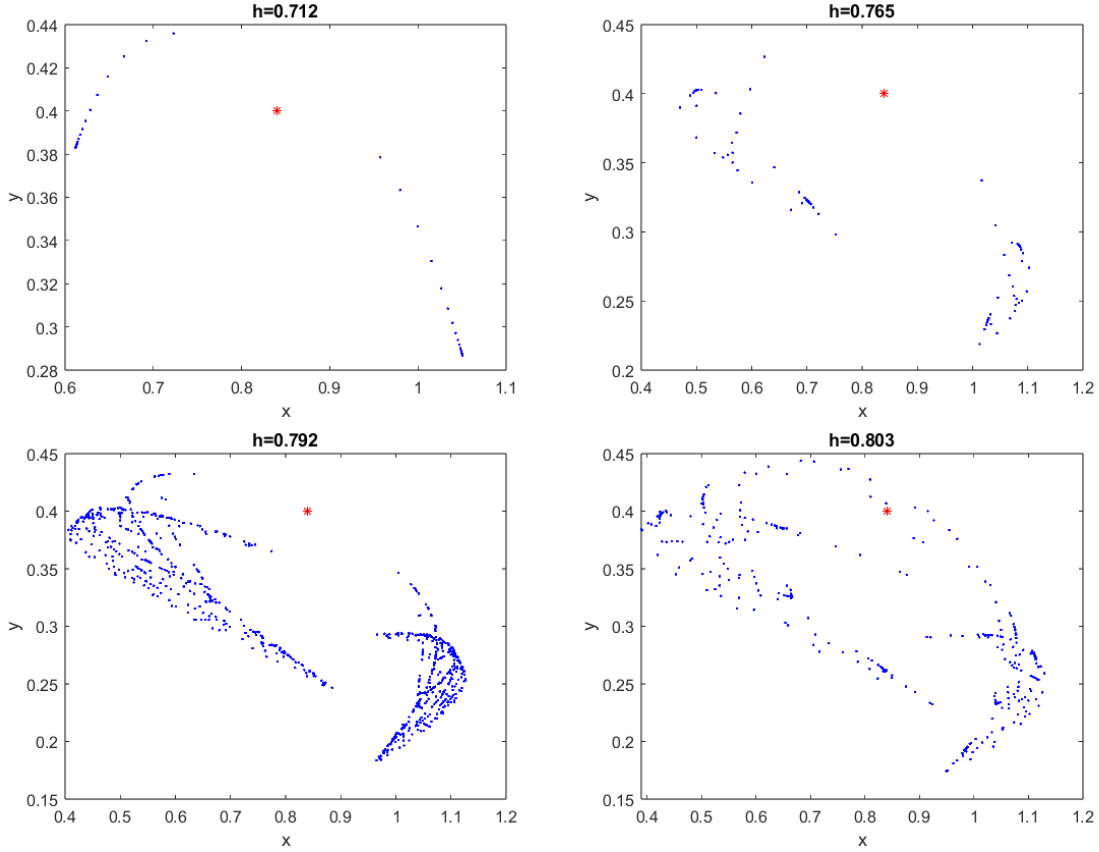


FIGURE 2. The phase diagram for altering the input of h . The fixed point is indicated by red *

Scenario (ii): In this scenario, we use the parameter values: $\eta_p = 2.7$, $\beta_p = 3.26$, $\delta_p = 1.5$, $\phi_p = 1.05$, $\gamma_p = 0.8$, $\tau = 0.5896$ and h varies between $0.5 \leq h \leq 1.2$. We arrive at a fixed point $\tilde{\xi}_3(x^*, y^*) = (0.645685, 0.506165)$ and a point $h_{NS} = 0.7013$ for NS bifurcation. The estimated eigenvalues are $\lambda_{1,2} = -0.375741 \pm 0.926724i$.

Also,

$$\frac{d|\lambda_i(h)|}{dh} \Big|_{h=h_{NS}} = 0.0493261 \neq 0$$

$$-(tr(U_{\tilde{\xi}_3})) \Big|_{h=h_{NS}} = -0.751482 \neq 0, 1.$$

Consider the two eigenvectors of $A(h_{NS})$ and $A^T(h_{NS})$, be $\tilde{q}_a, \tilde{q}_b \in \mathbb{C}^2$ which correspond to $\lambda_{1,2}$. Therefore,

$$\tilde{q}_a \sim (-0.143775 + 0.520139i, 0.841893)^T \text{ and } \tilde{q}_b \sim (0.841893, 0.143775 - 0.520139i)^T.$$

For $\langle \tilde{q}_a, \tilde{q}_b \rangle = 1$, after which the normalized vector can be used as $\tilde{q}_b = \vartheta_{NS} \tilde{q}_b$ where, $\vartheta_{NS} = -1.80929 \times 10^{-16} + 1.14181i$. Also, the Taylor coefficients are obtained as follows by using Eq.(15).

$$\begin{aligned} \hat{h}_{20}(h_{NS}) &= -1.02373 + 0.951245i, \\ \hat{h}_{11}(h_{NS}) &= -1.03832 + 0.828311i, \\ \hat{h}_{02}(h_{NS}) &= -1.0529 - 2.13156i, \\ \hat{h}_{21}(h_{NS}) &= 0.968173 - 5.98468i. \end{aligned}$$

The Lyapunov coefficient $s_2(h_{NS}) = -4.19732 > 0$ is obtained from (16). As a result, Theorem 2 is established, and the bifurcation is NS, which is super-critical.

The parameter h is utilized to generate the bifurcation diagram (NS) for the system (4). Figure 3 depicts the NS bifurcation. The phase portraits are shown in Figure 4 corresponding to Figure 3 (a,b) for several choices of h demonstrating how the smooth invariant curve behaves as it grows in radius and separates from the stable fixed point. We have also explored NS bifurcation; Figure 5 displays the corresponding NS bifurcation diagrams. To do this, the fractional order τ was changed within the range $0.02 \leq \tau \leq 0.8$, while all other parameters for Figure 3 were fixed with $h = 0.7013$.

Scenario (iii): If other parameter values alter (for example, the parameter β_p), the proposed model in the NS bifurcation diagram may have more dynamic behavior. The following values are used to generate a new NS diagram: $\eta_p = 2.7$, $h = 0.7013$, $\delta_p = 1.5$, $\phi_p = 1.05$, $\gamma_p = 0.8$, $\tau = 0.5896$ and β_p varies between $3.1 \leq \beta_p \leq 3.8$, as depicted in Figure 6 (a-b). The model has a Neimark-Sacker bifurcation at $\beta_{pNS} = 3.26$.

6.1. Biological Implications. In discrete prey-predator models, bifurcations can have important ecological ramifications. The relationships between a group of animals that hunt and another group of animals that hunting are explained by these models. The animals that hunt are the ones that consume the prey in these models.

Neimark-Sacker and period-doubling bifurcations are phenomena observed in dynamical systems, such as ecological models. These splits can provide insight into the complexity and stability of ecological systems, and they have important biological ramifications. In population

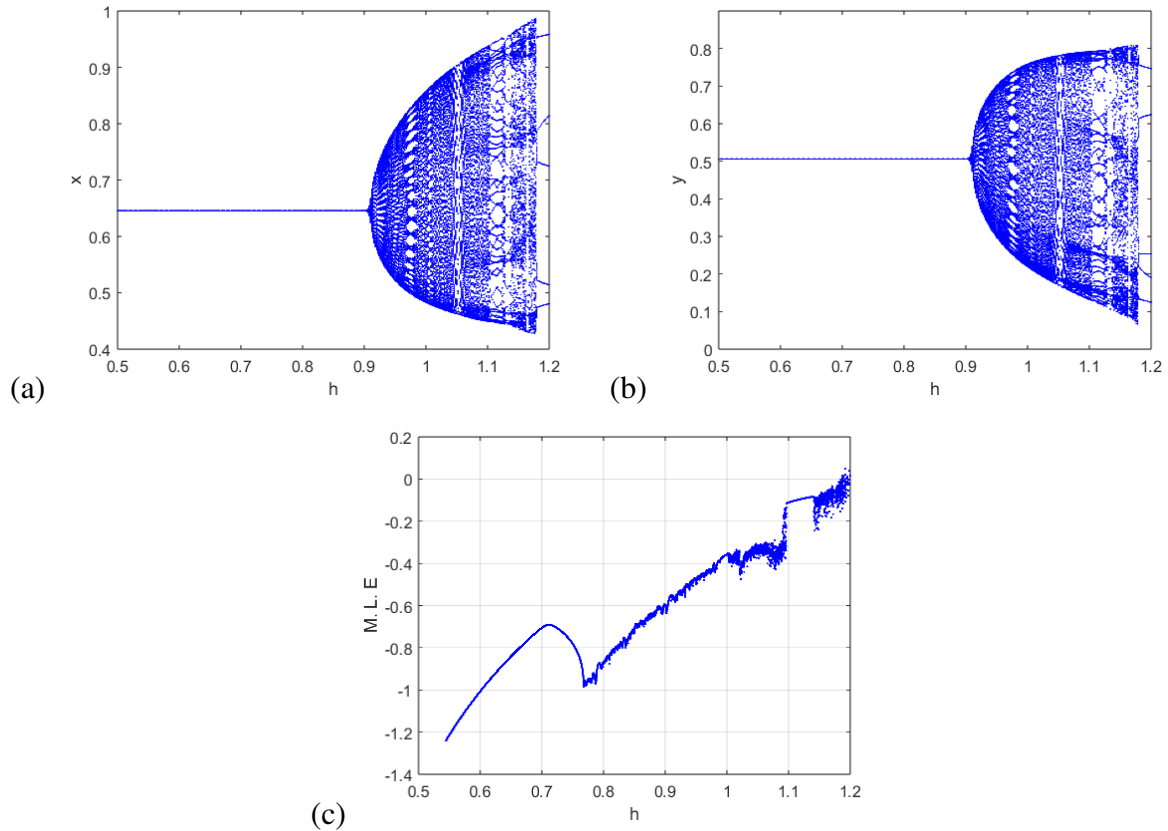


FIGURE 3. Visualisation of NS bifurcation and MLEs of species for changing parameter h

dynamics, period-doubling bifurcations are characterised by the doubling of the oscillation period, which can have important ecological ramifications. Period-doubling bifurcations often signify the transition of a system's dynamics from regular, predictable patterns to random ones. In the context of ecological models, this change may indicate a decline in predictive capacity and the emergence of complex, stochastic population level fluctuations. Period-doubling bifurcations are associated with the generation of stable cycles of different lengths that make up periodic orbits. From an ecological point of view, this can be understood as the oscillation between distinct population cycles, such as the periodic oscillations of populations of predators and prey with differing lengths. Through the analysis of these models, we can gain insight into the basic principles governing population cycles and other ecological processes, and develop more effective strategies to improve the stability and resilience of ecosystems.

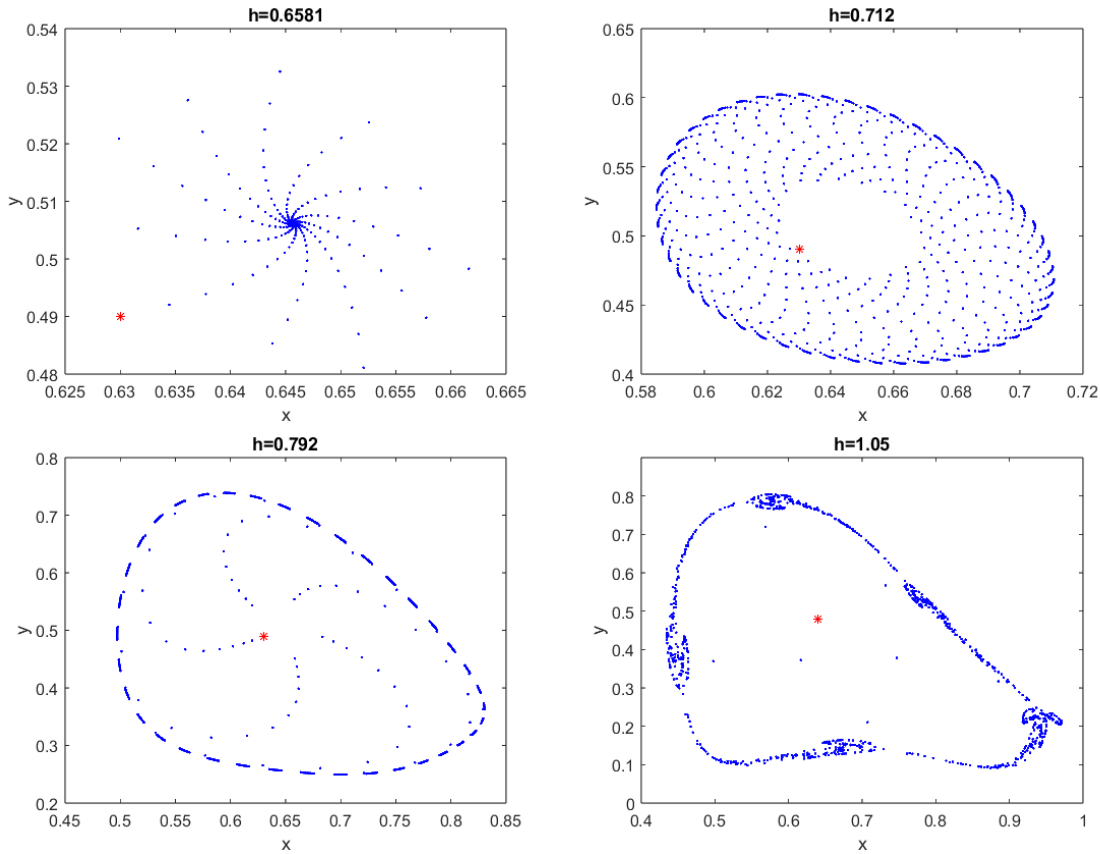


FIGURE 4. The phase diagram for altering the input of h . The fixed point is indicated by a red *

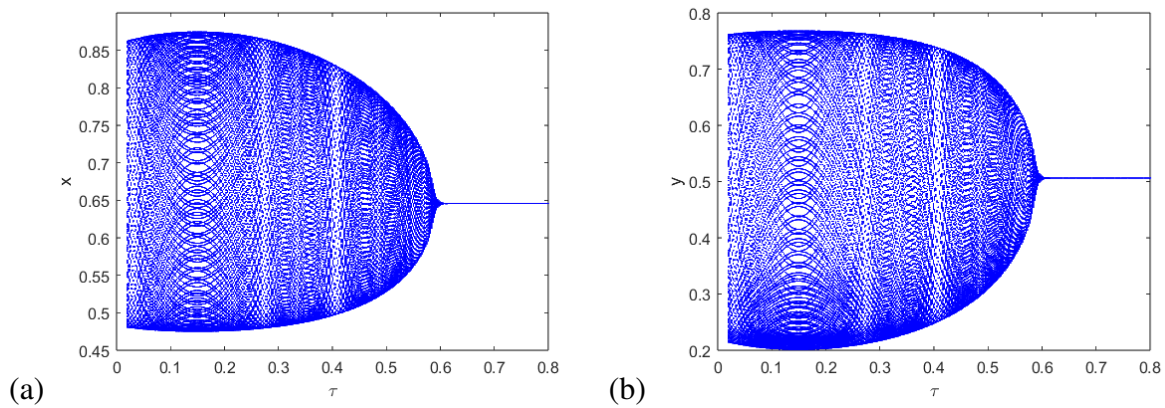


FIGURE 5. Visualisation of NS Bifurcation of species for changing fractional order τ

In dynamical systems, the transition from periodic to quasi-periodic behaviour is associated with Neimark-Sacker bifurcations. This may signal a shift in ecological models from simple, repeatable population cycles to more intricate, non-repetitive patterns. The ecological system

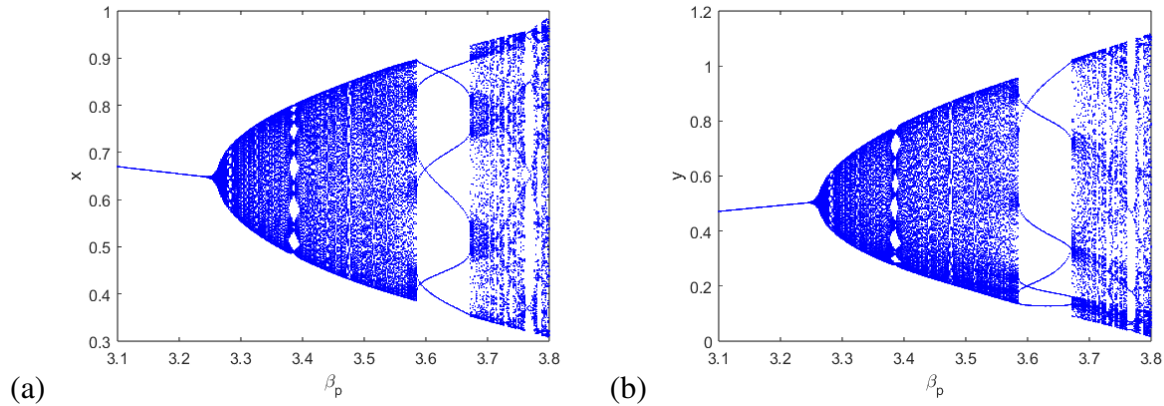


FIGURE 6. Visualisation of NS Bifurcation of species for changing parameter β_p

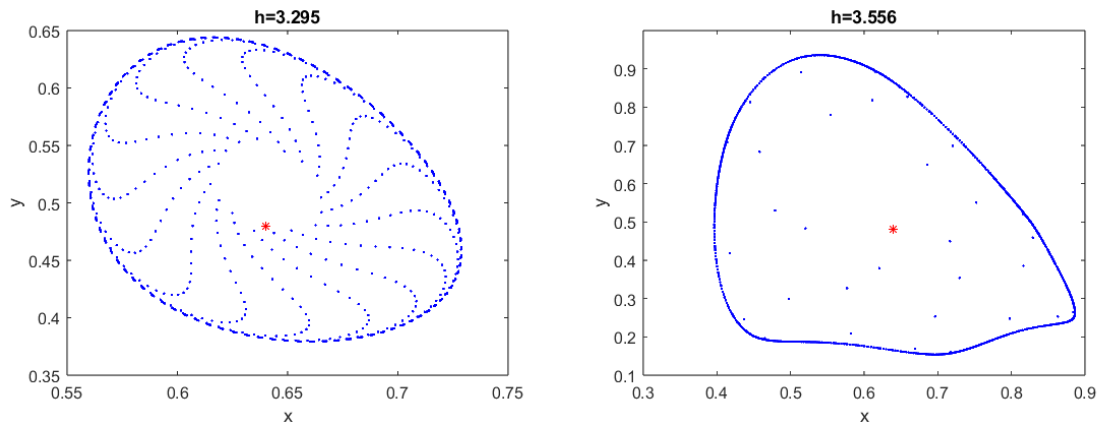


FIGURE 7. The phase diagram for altering the input of β_p . The fixed point is indicated by a red *

experiences quasi-periodic oscillations when Neimark-Sacker bifurcations are present. The oscillations are not exactly repeated, which increases the complexity of the temporal dynamics of interacting species. Neimark-Sacker bifurcation in discrete prey-predator models generally highlights how important it is to understand population dynamics and interactions in ecological systems. We may learn more about the underlying mechanisms underlying population cycles and other ecological processes by examining these models. We can also use this knowledge to create more potent policies aimed at enhancing the resilience and stability of ecosystems.

7. CHAOS MANAGEMENT

Because dynamical systems avoid chaos, they are considered the best method for chaos control based on a performance criterion. Numerous academic fields, including physics, biology, ecology, and telecommunications, study chaotic behavior. Effective chaos management approaches can be also applied in a wide range of industries, such as physics labs, biochemistry, cardiology, turbulence, and communication systems. Managing chaos dynamics in discrete-time systems has drawn the attention of numerous scientists in recent times.

In this part, we will apply Ott-Grebogi-Yorke (OGY) [26] feedback control and a hybrid control technique to system (4) in order to prevent chaos at the positive fixed point of system (4) due to Neimark-Sacker bifurcation. We write system (4) as follows:

$$(17) \quad \begin{aligned} x_{n+1} &= x_n + \frac{h^\tau}{\Gamma(\tau+1)} (\delta_p x_n (1-x_n) - \phi_p x_n y_n) = g_{p1}(x, y, \beta_p), \\ y_{n+1} &= y_n + \frac{h^\tau}{\Gamma(\tau+1)} (\beta_p x_n y_n + (1-\eta_p) y_n - \gamma_p y_n^2) = g_{p2}(x, y, \beta_p). \end{aligned}$$

where β_p is assumed to be the prominent parameter for eliminating chaos. Moreover, it is considered that $\beta_p \in (\beta_{p0} - \delta_1, \beta_{p0} + \delta_1)$ with $\delta_1 > 0$ and β_{p0} denoting the nominal value of β_p . In the neighbourhood of the fixed point $\zeta_3(x^*, y^*)$, where $x^* = \frac{\gamma_p \delta_p + (-1 + \eta_p) \phi_p}{\gamma_p \delta_p + \beta_p \phi_p}$ and $y^* = \frac{\delta_p (1 + \beta_p - \eta_p)}{\gamma_p \delta_p + \beta_p \phi_p}$, one can approximate system (17) as

$$(18) \quad \begin{bmatrix} x_{n+1} - x^* \\ y_{n+1} - y^* \end{bmatrix} \approx \tilde{A}_{cc} \begin{bmatrix} x_n - x^* \\ y_n - y^* \end{bmatrix} + \tilde{B}_{cc} [\beta_p - \beta_{p0}],$$

where

$$\begin{aligned} \tilde{A}_{cc} &= \begin{bmatrix} \frac{\partial g_{p1}(x, y, \beta_p)}{\partial x} & \frac{\partial g_{p1}(x, y, \beta_p)}{\partial y} \\ \frac{\partial g_{p2}(x, y, \beta_p)}{\partial x} & \frac{\partial g_{p2}(x, y, \beta_p)}{\partial y} \end{bmatrix} \\ &= \begin{bmatrix} \frac{\gamma_p (\delta_p - \delta_p^2 \mu_{dd}) + (\beta_p - \delta_p) (-1 + \eta_p) \mu_{dd} \phi_p}{\gamma_p \delta_p + \beta_p \phi_p} & \frac{-\mu_{dd} \phi_p (\gamma_p \delta_p + (-1 + \eta_p) \phi_p)}{\gamma_p \delta_p + \beta_p \phi_p} \\ \frac{\beta_p \delta_p (1 + \beta_p - \eta_p) \mu_{dd}}{\gamma_p \delta_p + \beta_p \phi_p} & \frac{-\gamma_p \delta_p (-1 + (1 + \beta_p - \eta_p) \mu_{dd}) + \beta_p \phi_p}{\gamma_p \delta_p + \beta_p \phi_p} \end{bmatrix}, \end{aligned}$$

and

$$\tilde{B}_{cc} = \begin{bmatrix} \frac{\partial g_{p1}(x, y, \beta_p)}{\partial \beta_p} \\ \frac{\partial g_{p2}(x, y, \beta_p)}{\partial \beta_p} \end{bmatrix} = \begin{bmatrix} 0 \\ \frac{\delta_p (1 + \beta_p - \eta_p) \mu_{dd} (\gamma_p \delta_p + (-1 + \eta_p) \phi_p)}{(\gamma_p \delta_p + \beta_p \phi_p)^2} \end{bmatrix}$$

As a result, the controllability matrix of the system (17) is as follows:

$$\begin{aligned} \tilde{C}_{cc} &= \left[\tilde{B}_{cc} : \tilde{A}_{cc}\tilde{B}_{cc} \right] \\ &= \left[\begin{array}{cc} 0 & \frac{-\delta_p(1+\beta_p-\eta_p)\tilde{\mu}_{dd}^2\phi_p(\gamma_p\delta_p+(-1+\eta_p)\phi_p)^2}{(\gamma_p\delta_p+\beta_p\phi_p)^3} \\ \frac{\delta_p(1+\beta_p-\eta_p)\tilde{\mu}_{dd}(\gamma_p\delta_p+(-1+\eta_p)\phi_p)}{(\gamma_p\delta_p+\beta_p\phi_p)^2} & \frac{-\delta_p(1+\beta_p-\eta_p)\tilde{\mu}_{dd}(\gamma_p\delta_p+(-1+\eta_p)\phi_p)-\beta_p\phi_p(\gamma_p\delta_p+(-1+\eta_p)\phi_p)}{(\gamma_p\delta_p+\beta_p\phi_p)^3} \end{array} \right] \end{aligned}$$

So, it is simple to establish that \tilde{C}_{cc} has a rank of 2. We imagine that

$$\begin{aligned} [\beta_p - \beta_{p0}] &= -\tilde{K}_{cc} \begin{bmatrix} x_n - x^* \\ y_n - y^* \end{bmatrix} \text{ where } \tilde{K}_{cc} = [\tilde{\sigma}_{c1} \quad \tilde{\sigma}_{c2}], \text{ then system (17) becomes} \\ &\begin{bmatrix} x_{n+1} - x^* \\ y_{n+1} - y^* \end{bmatrix} \approx [\tilde{A}_{cc} - \tilde{B}_{cc}\tilde{K}_{cc}] \begin{bmatrix} x_n - x^* \\ y_n - y^* \end{bmatrix} \end{aligned}$$

Furthermore, system (4) provides the appropriate controlled system, which is

$$\begin{aligned} (19) \quad x_{n+1} &= x_n + \frac{h^\tau}{\Gamma(\tau+1)} (\delta_p x_n (1-x_n) - \phi_p x_n y_n), \\ y_{n+1} &= y_n + \frac{h^\tau}{\Gamma(\tau+1)} ((\beta_{p0} - \tilde{\sigma}_{c1}(x_n - x^*) - \tilde{\sigma}_{c2}(y_n - y^*))x_n y_n + (1 - \eta_p)y_n - \gamma_p y_n^2). \end{aligned}$$

Moreover,

$$\tilde{A}_{cc} - \tilde{B}_{cc}\tilde{K}_{cc} = \begin{bmatrix} \tilde{b}_{11} & \tilde{b}_{12} \\ \tilde{b}_{21} & \tilde{b}_{22} \end{bmatrix},$$

where

$$\begin{aligned} \tilde{b}_{11} &= 1 + \tilde{\mu}_{dd} \left(-\frac{\delta_p(1+\beta_p-\eta_p)\phi_p}{\gamma_p\delta_p+\beta_p\phi_p} - \frac{\delta_p(\gamma_p\delta_p+(-1+\eta_p)\phi_p)}{\gamma_p\delta_p+\beta_p\phi_p} + \delta_p \left(1 - \frac{\gamma_p\delta_p+(-1+\eta_p)\phi_p}{\gamma_p\delta_p+\beta_p\phi_p} \right) \right) \\ \tilde{b}_{12} &= -\frac{\tilde{\mu}_{dd}\phi_p(\gamma_p\delta_p+(-1+\eta_p)\phi_p)}{\gamma_p\delta_p+\beta_p\phi_p} \\ \tilde{b}_{21} &= \frac{\beta_p\delta_p(1+\beta_p-\eta_p)\tilde{\mu}_{dd}}{\gamma_p\delta_p+\beta_p\phi_p} - \frac{\delta_p(1+\beta_p-\eta_p)\tilde{\mu}_{dd}(\gamma_p\delta_p+(-1+\eta_p)\phi_p)\tilde{\sigma}_{c1}}{(\gamma_p\delta_p+\beta_p\phi_p)^2} \\ \tilde{b}_{22} &= 1 + \tilde{\mu}_{dd} \left(1 - \eta_p - \frac{2\gamma_p\delta_p(1+\beta_p-\eta_p)}{\gamma_p\delta_p+\beta_p\phi_p} + \frac{\beta_p(\gamma_p\delta_p+(-1+\eta_p)\phi_p)}{\gamma_p\delta_p+\beta_p\phi_p} \right) \\ &\quad - \frac{\delta_p(1+\beta_p-\eta_p)\tilde{\mu}_{dd}(\gamma_p\delta_p+(-1+\eta_p)\phi_p)\tilde{\sigma}_{c2}}{(\gamma_p\delta_p+\beta_p\phi_p)^2} \end{aligned}$$

Furthermore,

$$(20) \quad \lambda_c^2 - \tilde{\Lambda}_{bb}\lambda_c + \tilde{F}_{bb} = 0,$$

where

$$(21) \quad \begin{aligned} \tilde{\Lambda}_{bb} &= \tilde{b}_{11} + \tilde{b}_{22}, \\ \tilde{F}_{bb} &= \tilde{b}_{11}\tilde{b}_{22} - \tilde{b}_{12}\tilde{b}_{21}. \end{aligned}$$

Thus, the lines of marginal stability may be obtained by solving the equations $\lambda_{c1} = \pm 1$ and $\lambda_{c1}\lambda_{c2} = 1$. The eigenvalues of open unit disc also guarantee adherence to these constraints. We derive the following equations from Eq.(20), taking into account the situations $\lambda_{c1}\lambda_{c2} = 1$, $\lambda_{c1} = -1$ and $\lambda_{c1} = 1$ sequentially.

$$\begin{aligned} L_{b1} &= \tilde{F}_{bb} - 1, \\ L_{b2} &= \tilde{\Lambda}_{bb} - \tilde{F}_{bb} - 1, \\ L_{b3} &= 1 + \tilde{\Lambda}_{bb} + \tilde{F}_{bb}. \end{aligned}$$

As a result, the stability zone for system(17) in the $\tilde{\sigma}_{c1}, \tilde{\sigma}_{c2}$ -plane form a triangle bordered by L_{b1}, L_{b2} and L_{b3} .

To avoid an NS bifurcation in a discrete model operating in discrete time, the authors of [35] used a hybrid control strategy. In the prey-predator model with fractional order, we propose a hybrid control method for controlling a NS bifurcation. A hybrid control approach is used to control chaos in the system (4). We modify our uncontrolled system (4) as follows:

$$(22) \quad X_{n+1} = \tilde{G}(X_n, \tau, h)$$

where $X_n \in \mathbb{R}^2$, $\tilde{G}(\cdot)$ is a nonlinear vector function and $\tau, h \in \mathbb{R}$ is a bifurcation parameter. When the hybrid control technique is utilized, the controlled system (22) becomes

$$(23) \quad X_{n+1} = \omega_p \tilde{G}(X_n, \tau, h) + (1 - \omega_p)X_n,$$

where ω_p denotes as the parameter to eliminate chaos. When we impose a control strategy described above to the system (4), we obtain,

$$(24) \quad \begin{aligned} x_{n+1} &= \omega_p \left(x_n + \frac{h^\tau}{\Gamma(\tau+1)} (\delta_p x_n (1-x_n) - \phi_p x_n y_n) \right) + (1 - \omega_p)x_n, \\ y_{n+1} &= \omega_p \left(y_n + \frac{h^\tau}{\Gamma(\tau+1)} (\beta_p x_n y_n + (1 - \eta_p)y_n - \gamma_p y_n^2) \right) + (1 - \omega_p)y_n. \end{aligned}$$

Scenario (iv): We now investigate the OGY of system (4) by setting $(\eta_p, \delta_p, \phi_p, \gamma_p, \beta_{p0}, \tau, h) = (2.7, 1.5, 1.05, 0.8, 3.6, 0.5896, 0.7013)$. System (4) is unstable in this case and has a single non-negative fixed point $(x^*, y^*) = (0.599398, 0.572289)$. The controlled system is then given by,

$$(25) \quad \begin{aligned} x_{n+1} &= x_n + 0.909032 (1.5x_n(1 - x_n) - 1.05x_ny_n), \\ y_{n+1} &= y_n + 0.909032 ((3.6 - \tilde{\sigma}_{c1}(x_n - x^*) - \tilde{\sigma}_{c2}(y_n - y^*))x_ny_n + (1 - 2.7)y_n - 0.8y_n^2), \end{aligned}$$

where $\tilde{K} = [\tilde{\sigma}_{b1} \quad \tilde{\sigma}_{b2}]$. We also obtain,

$$\begin{aligned} \tilde{A}_{cc} &= \begin{bmatrix} 0.182693 & -0.572115 \\ 1.87282 & 0.583817 \end{bmatrix}, \\ \tilde{B}_{cc} &= \begin{bmatrix} 0 \\ 0.311824 \end{bmatrix}, \\ \tilde{C}_{cc} &= \begin{bmatrix} 0 & -0.178399 \\ 0.311824 & 0.182048 \end{bmatrix}. \end{aligned}$$

The rank of the matrix \tilde{C}_{cc} is then proved to be 2. As a result, the system (25) can be controlled, and the identifying matrix of the managed system is provided by,

$$\tilde{A}_{cc} - \tilde{B}_{cc}\tilde{K}_{cc} = \begin{bmatrix} 0.182693 & -0.572115 \\ 1.87282 - 0.311824\tilde{\sigma}_{c1} & 0.573817 - 0.311824\tilde{\sigma}_{c2} \end{bmatrix}.$$

Also,

$$L_{b1} = 0.178131 - 0.178399\tilde{\sigma}_{c1} - 0.056968\tilde{\sigma}_{c2} = 0,$$

$$L_{b2} = -1.41162 + 0.178399\tilde{\sigma}_{c1} - 0.254856\tilde{\sigma}_{c2} = 0,$$

$$L_{b3} = 2.94464 - 0.178399\tilde{\sigma}_{c1} - 0.368792\tilde{\sigma}_{c2} = 0.$$

The stable triangular zone for the regulated system (25) is thus represented in Figure 8.

Scenario (v): To determine the efficiency of the hybrid control strategy in minimizing chaotic scenarios, we use the parameter values described for the OGY technique except $h = 0.5699 < h_{NS}$. As a consequence, it shows that the fixed point $\tilde{\zeta}_3(x^*, y^*) = (0.599398, 0.572289)$ of the system (4) is unstable, whereas for the regulated system (24), $\tilde{\zeta}_3$ will be stable if $0 < \omega_p < 0.5499$. By taking $\omega_p = 1.01393$, we can see that the controlled system (24) has a fixed point

$\tilde{\zeta}_3(x^*, y^*)$ that acts as a sink, eliminate irregular behavior around $\tilde{\zeta}_3(x^*, y^*)$. The phase image and stable trajectories are depicted in Figure 9. Furthermore, we present the NS bifurcation diagrams (Figure 10) of the controlled system (24) for various values of ω_p and show that the system is under control when $\omega_p = 0.5499$.

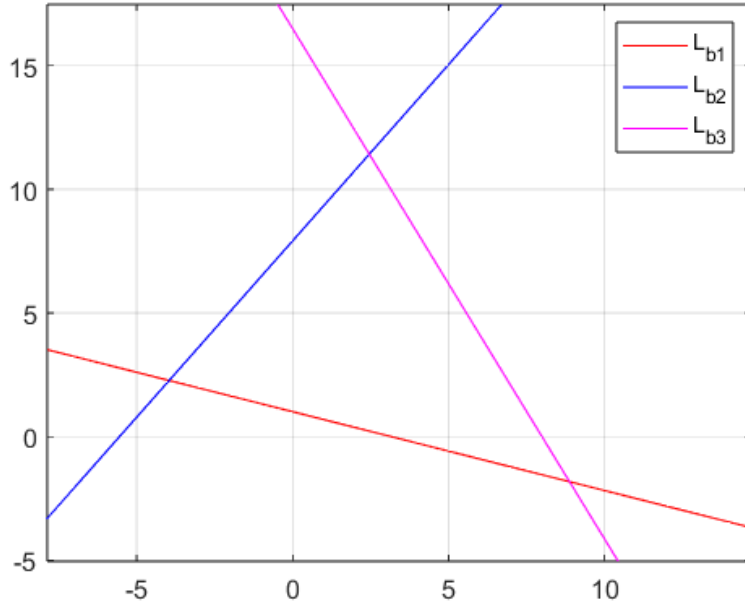


FIGURE 8. Stable zone created by OGY method

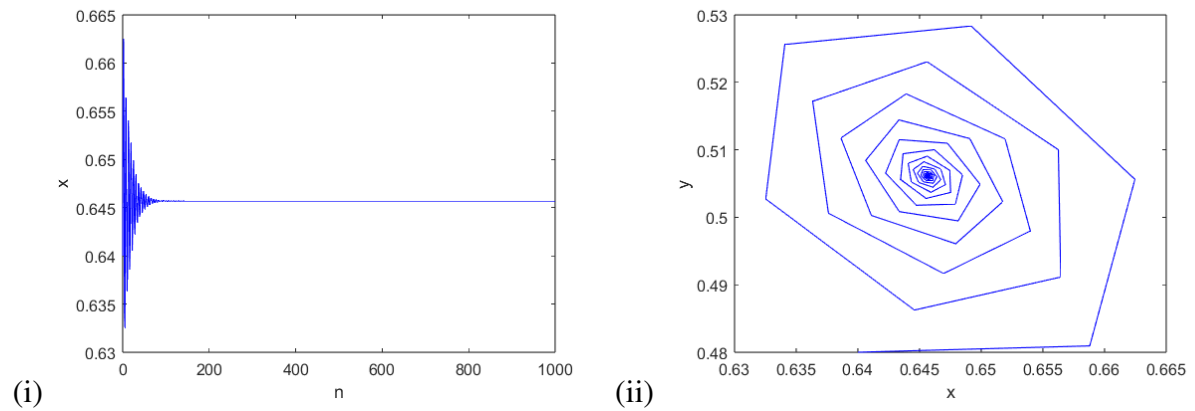


FIGURE 9. Controlling chaos of the uncontrolled system (17) (i) Time trajectory (ii) Phase picture

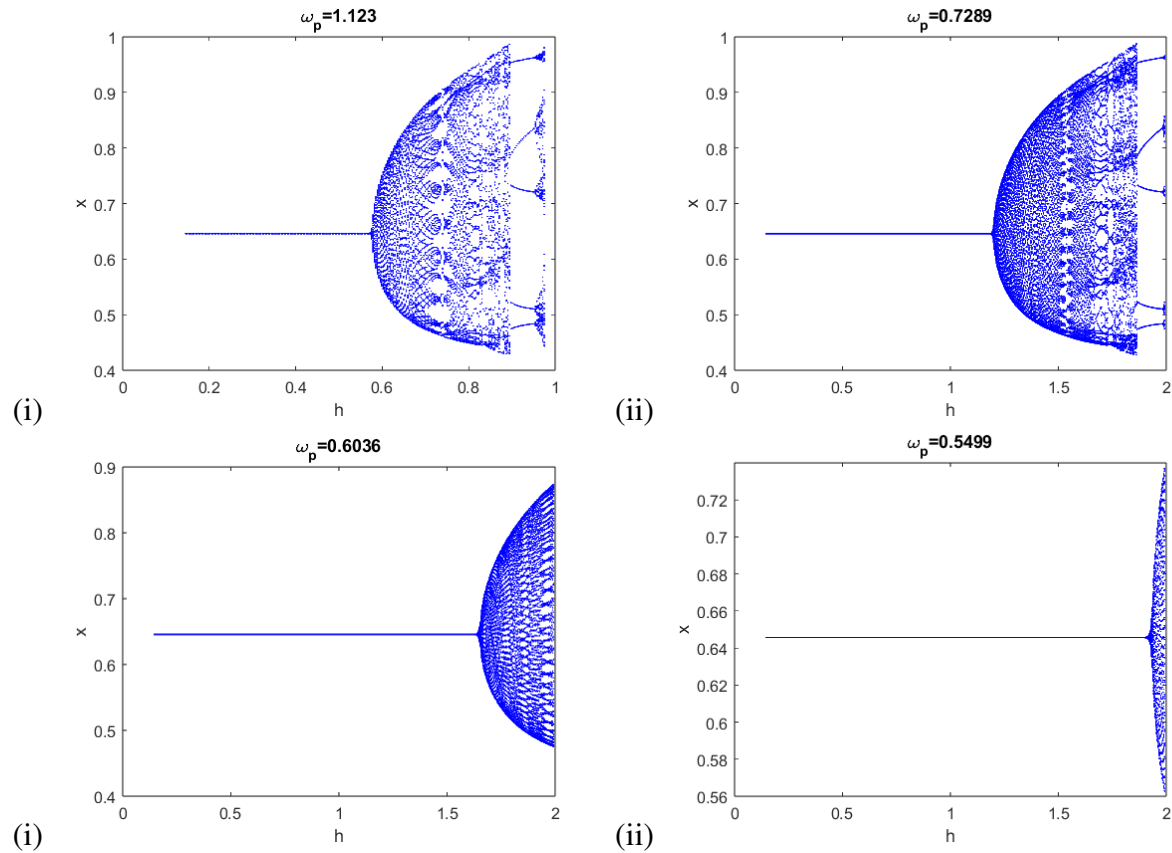


FIGURE 10. NS bifurcation in prey populations for (i) $\omega_p = 1.123$, (ii) $\omega_p = 0.7289$, (iii) $\omega_p = 6036$, (iv) $\omega_p = 0.5499$

8. DISCUSSIONS

This paper has investigated the dynamics of a discrete model of prey and predator with fractional-order intraspecific competition. Under certain parametric conditions, four fixed points have been found, and the stability of these fixed points is discussed in detail throughout the article. We have shown both analytically and computationally that, under specific circumstances, the model system can experience Neimark-Sacker bifurcations and period-doubling bifurcations. We have observed that the model parameters significantly impact the stability of the fixed points. Notably, our results show that the model exhibits chaotic behavior and the system destabilizes with increasing parameters h, β_p splitting the system into chaotic and stable states. The dynamic behavior of the proposed system with varying levels of complexity is revealed by the existence of distinct bifurcations from various angles. For example, the NS bifurcation initiates a way toward chaos by generating a vibrant transition from a stable position to appealing

cycles, leading to the emergence of complex dynamics including chaotic attractors and periodic windows. Environmental changes can cause populations with irregular oscillations to suddenly transition to ones with regular oscillations. Crucial information about nonlinear systems can be gained from the invariant curve in the supercritical Neimark-Sacker bifurcation. It is essential to comprehend the shift from a periodic position to complex dynamics because it shows how the system behaves when the parameter changes. A curve for supercritical NS in ecology indicates that populations of both predator and prey may coexist and self-produce. There may be quasi-periodic or periodic dynamics on the invariant curve. A PD bifurcation in the model illustrates how the populations of predators and prey have evolved. The evolution of chaotic nature from a stable position is linked to the PD bifurcation. It illustrates the diversity and pervasiveness of chaotic nature in a range of natural systems and occurrences. Additionally, we demonstrate the numerical and analytical result of the OGY and hybrid control strategies to eliminate chaotic scenarios.

Our key conclusion is that the term memory which is represented by the parameter τ has a considerable effect on the behavior of the system. According to our findings, a feeble memory is indicated by a τ value that is going close to 1, which causes chaotic behavior. On the other hand, an intense memory is indicated by a τ value that is approaching zero, which makes the system stable. These results highlight the critical role memory plays in the model's behavior. In conclusion, this work provides a thorough examination of dynamic behavior of the proposed model and demonstrates how, under specific parametric circumstances, bifurcations and chaos might arise. We also show how system behavior is influenced by memory.

FUNDING

This project was partially funded by RND project of the Govt. of Bangladesh.

DATA AVAILABILITY STATEMENT

There are no related data for this manuscript.

ACKNOWLEDGEMENT

We want to acknowledge RND project of Bangladesh.

AUTHORS' CONTRIBUTIONS

The main findings were verified by all authors, who also gave their unanimous approval to the final manuscript.

CONFLICT OF INTERESTS

The authors declare that there is no conflict of interests.

REFERENCES

- [1] D. Hu, H. Cao, Bifurcation and chaos in a discrete-time predator-prey system of Holling and Leslie type, *Commun. Nonlinear Sci. Numer. Simul.* 22 (2015), 702–715. <https://doi.org/10.1016/j.cnsns.2014.09.010>.
- [2] S.M. Salman, A.M. Yousef, A.A. Elsadany, Stability, bifurcation analysis and chaos control of a discrete predator-prey system with square root functional response, *Chaos Solitons Fractals*. 93 (2016), 20–31. <https://doi.org/10.1016/j.chaos.2016.09.020>.
- [3] Q. Din, Complexity and chaos control in a discrete-time prey-predator model, *Commun. Nonlinear Sci. Numer. Simul.* 49 (2017), 113–134. <https://doi.org/10.1016/j.cnsns.2017.01.025>.
- [4] M.B. Ajaz, U. Saeed, Q. Din, et al. Bifurcation analysis and chaos control in discrete-time modified Leslie-Gower prey harvesting model, *Adv. Differ. Equ.* 2020 (2020), 45. <https://doi.org/10.1186/s13662-020-2498-1>.
- [5] G.C. Layek, *An introduction to dynamical systems and chaos*, Springer, New Delhi, 2015. <https://doi.org/10.1007/978-81-322-2556-0>.
- [6] K.P. Hadeler, I. Gerstmann, The discrete Rosenzweig model, *Math. Biosci.* 98 (1990), 49–72. [https://doi.org/10.1016/0025-5564\(90\)90011-m](https://doi.org/10.1016/0025-5564(90)90011-m).
- [7] L. Cheng, H. Cao, Bifurcation analysis of a discrete-time ratio-dependent predator–prey model with Allee Effect, *Commun. Nonlinear Sci. Numer. Simul.* 38 (2016), 288–302. <https://doi.org/10.1016/j.cnsns.2016.02.038>.
- [8] X. Liu, D. Xiao, Complex dynamic behaviors of a discrete-time predator-prey system, *Chaos Solitons Fractals*. 32 (2007), 80–94. <https://doi.org/10.1016/j.chaos.2005.10.081>.
- [9] W. Ishaque, Q. Din, M. Taj, et al. Bifurcation and chaos control in a discrete-time predator-prey model with nonlinear saturated incidence rate and parasite interaction, *Adv. Differ. Equ.* 2019 (2019), 28. <https://doi.org/10.1186/s13662-019-1973-z>.
- [10] M.A. Khan, Chaotic behavior of harvesting Leslie-Gower predator-prey model, *Comput. Ecol. Softw.* 9 (2019), 67–88.

- [11] M.A.M. Abdelaziz, A.I. Ismail, F.A. Abdullah, et al. Bifurcations and chaos in a discrete SI epidemic model with fractional order, *Adv. Differ. Equ.* 2018 (2018), 44. <https://doi.org/10.1186/s13662-018-1481-6>.
- [12] W.M. Ahmad, J.C. Sprott, Chaos in fractional-order autonomous nonlinear systems, *Chaos Solitons Fractals.* 16 (2003), 339–351. [https://doi.org/10.1016/s0960-0779\(02\)00438-1](https://doi.org/10.1016/s0960-0779(02)00438-1).
- [13] E. Balci, I. Öztürk, S. Kartal, Dynamical behaviour of fractional order tumor model with Caputo and conformable fractional derivative, *Chaos Solitons Fractals.* 123 (2019), 43–51. <https://doi.org/10.1016/j.chaos.2019.03.032>.
- [14] A.A. Elsadany, A.E. Matouk, Dynamical behaviors of fractional-order Lotka-Volterra predator-prey model and its discretization, *J. Appl. Math. Comput.* 49 (2014), 269–283. <https://doi.org/10.1007/s12190-014-0838-6>.
- [15] A. Atangana, A. Secer, A note on fractional order derivatives and table of fractional derivatives of some special functions, *Abstr. Appl. Anal.* 2013 (2013), 279681. <https://doi.org/10.1155/2013/279681>.
- [16] A.J. Lotka, *Elements of physical biology*, Williams and Wilkins Company, Baltimore, (1925).
- [17] V. Volterra, *Variazioni e fluttuazioni del numero d'individui in specie animali conviventi*, Accademia dei Lincei, (1927).
- [18] R. Arditi, L.R. Ginzburg, Coupling in predator-prey dynamics: Ratio-Dependence, *J. Theor. Biol.* 139 (1989), 311–326. [https://doi.org/10.1016/s0022-5193\(89\)80211-5](https://doi.org/10.1016/s0022-5193(89)80211-5).
- [19] C. Cosner, D.L. DeAngelis, J.S. Ault, et al. Effects of spatial grouping on the functional response of predators, *Theor. Popul. Biol.* 56 (1999), 65–75. <https://doi.org/10.1006/tpbi.1999.1414>.
- [20] M. Danca, S. Codreanu, B. Bako, Detailed analysis of a nonlinear prey-predator model, *J. Biol. Phys.* 23 (1997), 11–20. <https://doi.org/10.1023/a:1004918920121>.
- [21] M. Fan, Y. Kuang, Dynamics of a nonautonomous predator-prey system with the Beddington-DeAngelis functional response, *J. Math. Anal. Appl.* 295 (2004), 15–39. <https://doi.org/10.1016/j.jmaa.2004.02.038>.
- [22] B. Liu, Y. Zhang, L. Chen, Dynamic complexities in a Lotka-Volterra predator-prey model concerning impulsive control strategy, *Int. J. Bifurcation Chaos.* 15 (2005), 517–531. <https://doi.org/10.1142/s0218127405012338>.
- [23] C.S. Holling, The functional response of predators to prey density and its role in mimicry and population regulation, *Mem. Entomol. Soc. Can.* 97 (1965), 5–60. <https://doi.org/10.4039/entm9745fv>.
- [24] M.O. AL-Kaff, H.A. El-Metwally, E.M.M. Elabbasy, Qualitative analysis and phase of chaos control of the predator-prey model with Holling type-III, *Sci. Rep.* 12 (2022), 20111. <https://doi.org/10.1038/s41598-022-23074-3>.
- [25] M.S. Khan, M. Samreen, J. Gómez-Aguilar, et al. On the qualitative study of a discrete-time phytoplankton-zooplankton model under the effects of external toxicity in phytoplankton population, *Heliyon.* 8 (2022), e12415. <https://doi.org/10.1016/j.heliyon.2022.e12415>.

- [26] E. Ott, C. Grebogi, J.A. Yorke, Controlling chaos, *Phys. Rev. Lett.* 64 (1990), 1196–1199. <https://doi.org/10.1103/physrevlett.64.1196>.
- [27] M. Caputo, Linear models of dissipation whose Q is almost frequency independent–II, *Geophys. J. Int.* 13 (1967), 529–539. <https://doi.org/10.1111/j.1365-246x.1967.tb02303.x>.
- [28] H. Sun, H. Cao, Bifurcations and chaos of a delayed ecological model, *Chaos Solitons Fractals.* 33 (2007), 1383–1393. <https://doi.org/10.1016/j.chaos.2006.01.089>.
- [29] M.J. Uddin, C.N. Podder, Fractional order prey-predator model incorporating immigration on prey: Complexity analysis and its control, *Int. J. Biomath.* 17 (2024), 2350051. <https://doi.org/10.1142/s1793524523500511>.
- [30] Y. Zhang, Q. Zhang, L. Zhao, C. Yang, Dynamical behaviors and chaos control in a discrete functional response model, *Chaos Solitons Fractals.* 34 (2007), 1318–1327. <https://doi.org/10.1016/j.chaos.2006.04.032>.
- [31] J. Guckenheimer, P. Holmes, Nonlinear oscillations, dynamical systems, and bifurcations of vector fields, Vol. 42, Applied Mathematical Sciences, Springer, New York, 2013. <https://doi.org/10.1007/978-1-4612-1140-2>.
- [32] Y.A. Kuznetsov, Elements of applied bifurcation theory, Vol. 112, Applied Mathematical Sciences, Springer, New York, 2004. <https://doi.org/10.1007/978-1-4757-3978-7>.
- [33] M.S. Khan, Bifurcation analysis of a discrete-time four-dimensional cubic autocatalator chemical reaction model with coupling through uncatalysed reactant, *MATCH Commun. Math. Comput. Chem.* 87 (2021), 415–439. <https://doi.org/10.46793/match.87-2.415k>.
- [34] Q. Din, T. Donchev, D. Kolev, Stability, bifurcation analysis and chaos control in chlorine dioxide–iodine–malonic acid reaction, *MATCH Commun. Math. Comput. Chem.* 79 (2018), 577–606.
- [35] L. Yuan, Q. Yang, Bifurcation, invariant curve and hybrid control in a discrete-time predator–prey system, *Appl. Math. Model.* 39 (2015), 2345–2362. <https://doi.org/10.1016/j.apm.2014.10.040>.
- [36] M.J. Uddin, S.M.S. Rana, Chaotic dynamics of the fractional order Schnakenberg model and its control, *Math. Appl. Sci. Eng.* 4 (2023), 40–60. <https://doi.org/10.5206/mase/15355>.
- [37] S.M.S. Rana, M.J. Uddin, P.K. Santra, et al. Chaotic dynamics and control of a discrete-time Chen system, *Math. Probl. Eng.* 2023 (2023), 7795246. <https://doi.org/10.1155/2023/7795246>.
- [38] A.Q. Khan, S.A.H. Bukhari, M.B. Almatrafi, Global dynamics, Neimark-Sacker bifurcation and hybrid control in a Leslie’s prey-predator model, *Alexandria Eng. J.* 61 (2022), 11391–11404. <https://doi.org/10.1016/j.aej.2022.04.042>.
- [39] I. Seval, F. Kangalgil, On the analysis of stability, bifurcation, and chaos control of discrete-time predator-prey model with Allee effect on predator, *Hacetatepe J. Math. Stat.* 51 (2022), 404–420. <https://doi.org/10.15672/hujms.728889>.
- [40] M. Berkal, J.F. Navarro, Qualitative behavior of a chemical reaction system with fractional derivatives, *Rocky Mt. J. Math.* in press.

- [41] W.K. Purves, G.H. Orians, D. Sadava, et al. *Life: The science of biology*, Vol. II: evolution, diversity, and ecology, Sinauer Associates, Sunderland, (2003).
- [42] M. Clark, T. Wolcott, D. Wolcott, et al. Intraspecific interference among foraging blue crabs *Callinectes sapidus*: interactive effects of predator density and prey patch distribution, *Mar. Ecol. Prog. Ser.* 178 (1999), 69–78. <https://doi.org/10.3354/meps178069>.
- [43] S. Ray, M. Straškraba, The impact of detritivorous fishes on a mangrove estuarine system, *Ecol. Model.* 140 (2001), 207–218. [https://doi.org/10.1016/s0304-3800\(01\)00321-0](https://doi.org/10.1016/s0304-3800(01)00321-0).
- [44] M.J. Uddin, S.M.S. Rana, S. Işık, et al. On the qualitative study of a discrete fractional order prey-predator model with the effects of harvesting on predator population, *Chaos Solitons Fractals.* 175 (2023), 113932. <https://doi.org/10.1016/j.chaos.2023.113932>.